Astron. Astrophys. 161, 125–129 (1986)

ASTRONOMY AND ASTROPHYSICS

Non-radial instability of WR models

A. Noels and R. Scuflaire

Institut d'Astrophysique, Université de Liège, Avenue de Cointe 5, B-4200 Ougrée, Belgium

Received November 4, accepted December 16, 1985

Summary. The development of a H burning shell in a massive star evolving with mass loss triggers a phase of vibrational instability towards g^+ modes of non radial oscillations. The e-folding time is of the order of 1000 yr but the unstable phase lasts only about 5 times more. Although the periods seem in accordance with those observed in some WR stars, it is still not clear that such a short unstable phase could be responsible for the observed variability.

Key words: non-radial oscillations – Wolf-Rayet stars – vibrational instability

1. Introduction

It is now generally accepted that a small fraction of WR stars could be formed through the evolution of stars more massive than $80\,M_\odot$, if the mass loss during the main sequence phase is sufficient to reveal the CNO processed material at the surface before the end of core H burning. This could correspond to the onset of the WR phase and the beginning of an increased mass loss rate (Noels and Gabriel, 1981). Another suggestion (Maeder, 1985) is that the star, soon after the end of the MS phase, becomes a Hubble Sandage variable, according to its location in the HR diagram and its surface abundances. The mass loss rate is then of the order of $10^{-3}\,M_\odot$/yr, quickly bringing the star to the onset of the WR phase. From this point on, with mass loss rates of the order of those observed in WR stars, the chemical structure of the star becomes more and more homogeneous and in some cases, the star is nearly a pure helium star in the early stages of core He burning. If the mass at that time exceeds the critical mass for homogeneous He burning stars, of the order of $16\,M_\odot$ (Boury and Ledoux, 1965; Noels-Grötsch, 1967; Simon and Stothers, 1969, 1970; Stothers and Simon, 1970; Noels and Masereel, 1982; Noels and Magain, 1984), a vibrational instability towards radial pulsations occurs (Noels and Gabriel, 1981, 1984; Maeder, 1985). It has been suggested (Noels and Gabriel, 1981, 1984) that the effect of such an instability would be an enhancement of the mass loss rate which would lasts a significant part of the core He burning phase, reducing the time necessary to reveal at the surface, matter processed by He burning. This would be at least a partial answer to the very critical question of the ratio of WC to WN stars, which seems to be of the order of 0.8, a very large number in view of the theoretical aspect of forming WR stars. This instability could also be related to a variability whose presence in at least some WR stars seems to have become in the last few years a well established fact (Weller and Jeffers, 1979; Vreux, 1985; Vreux et al., 1985), although the periods, which are smaller than one hour, seem to be too small to match the observations. A hope to reduce this discrepancy is to consider g^+ modes of non radial oscillations. Of course, at first sight, the situation is less favourable for a vibrational instability in the non radial case because the amplitudes of $\delta T/T$, $\delta\varrho/\varrho$, $\delta P/P$ tend to zero at the center while they remain different from zero in the radial case (Simon, 1957). Looking at the destabilizing nuclear terms only, core burning models will be bad candidates for a non radial vibrational instability. So, one has to switch from core He burning models to H shell burning ones in order to search with a reasonable hope for an instability of nuclear origin. We have limited our present study to the case of a $100\,M_\odot$ star evolving with mass loss. Some properties of the models are given in Sect. 2. The method used to compute the g^+ modes of some selected models is described in Sect. 3, where results are presented in the most interesting cases. Section 4 is a discussion of the vibrational stability towards g^+ modes of low harmonics degree l.

Send offprint requests to: A. Noels

2. Stellar models

All the models tested for vibrational stability come from the evolutionary sequence of a $100\,M_\odot$ star with a population I initial chemical composition $X=0.7$, $Z=0.02$. Nuclear reaction rates for H burning and He burning are those given in Fowler et al. (1975) and the opacity coefficients are interpolated in tables computed from the "Astrophysical Opacity Library" (Huebner et al., 1977).

The mass loss rate is the following

$$\dot{M}=9.672\ 10^{-13}\,L^{1.2}\left(\frac{R}{M}\right)^{0.5}M_\odot/\mathrm{yr},$$

where L, R, and M are expressed in solar units. More details can be found in Noels and Gabriel (1981) but for the sake of comprehensiveness, we reproduce in Fig. 1, the evolutionary track in the HR diagram with the position of the models analysed in this study. The point marked WR is the onset of the WR phase, that is to say the appearance at the surface of CNO processed material. From that point on, the mass loss rate is multiplied by a factor 5. Table 1 gives some properties of the models pointed out in Fig. 1. m_{sh} and r_{sh} are the mass and the radius in fraction of the total mass and fraction of the surface radius of the maximum value of the nuclear energy generation rate in a H burning shell. $L_{\mathrm{He}}/L_{\mathrm{nuc}}$ represents the fraction of the total amount of nuclear energy coming from He burning only.

Model 1 corresponds to the near exhaustion of hydrogen at the center, which becomes exactly zero after the so-called second

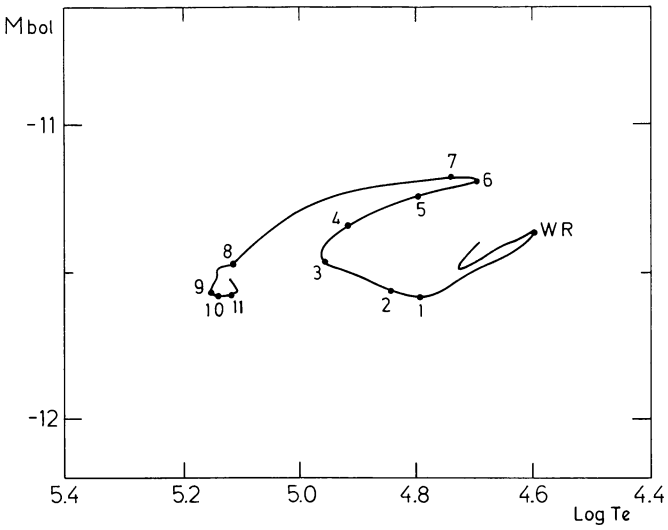

Fig. 1. Hertzsprung-Russell diagram

gravitational contraction, in model 3. From that model on, H is burnt in a shell while soon after, He burning starts in the core. Model 4 is especially interesting because it has an intermediate convective zone extending over nearly 6% of the total mass and located just after the maximum of nuclear energy generation rate. In model 5, more than half the total nuclear energy is generated through core He burning but, up to model 8, there is still enough H in the external layers to insure an efficient H shell burning. In model 8, the convective core reaches its maximum extent and then starts to decrease, due to the vanishing of the H burning shell.

Table 2. The first entry gives the period in hours, the second one, the damping time in years (a minus sign means amplicication) for the first few $l=1$ g^+ modes

	g_1^+	g_2^+	g_3^+	g_4^+
1	15.50	27.05	35.81	43.93
	2185	182.1	21.13	8.852
2	11.26	20.08	26.89	32.54
	2732	273.2	29.34	13.78
3	4.28	7.89	11.36	14.02
	-1853	4126	395.6	84.06
4	2.10	3.89	6.28	8.03
	2.907	-1326	29072	984.1
5	3.94	4.43	4.76	6.22
	0.1592	0.01886	27.08	201.8
6	5.75	6.70	6.91	8.11
	2.419	0.1821	0.8188	0.1921
7	5.16	5.46	5.94	6.88
	0.4695	5.825	0.06350	29.90
8	2.63	4.03	6.19	7.67
	4566	1032	65.20	20.99
9	2.14	3.52	4.67	6.39
	3846	1178	87.54	56.59
10	2.00	3.17	4.82	5.90
	3823	1633	128.3	26.41
11	1.93	2.97	4.41	5.22
	5046	1495	204.4	156.1

3. Non-radial adiabatic oscillations

The variables and equations used in the computation of non-radial, adiabatic modes are described in Boury et al (1975). The computed modes have been named according to the classification of Scuflaire (1974) and Osaki (1975). The validity of the criterion used in this classification has been proved by Gabriel and Scuflaire (1979, 1980) in the Cowling's approximation (when the perturbations of the gravitational potential are neglected). However, in the present case, this criterion did not work properly for the low

Table 1. Properties of the models

	$M/M_\odot$	$L/L_\odot$	$R/R_\odot$	T_e (K)	T_c (K)	ρ_c (g cm^{-3})	$\rho_c/\bar{\rho}$	m_{sh}	r_{sh}	L_{He}/L_{nuc}	Y_c	Y_s	t (yr)
WR	80.25	1.470(6)	25.95	39747	4.552(7)	2.022	312.4			0.	0.763	0.285	2.091(6)
1	41.44	1.198(6)	9.473	62417	5.971(7)	6.012	87.6			0.	0.978	0.855	2.708(6)
2	41.10	1.221(6)	7.664	69727	7.296(7)	1.102(1)	85.7			0.	0.980	0.860	2.716(6)
3	41.02	1.335(6)	4.806	90033	1.261(8)	5.746(1)	110.4			0.	0.980	0.861	2.718(6)
4	40.94	1.503(6)	6.155	82111	1.717(8)	1.527(2)	617.5	0.853	0.206	0.219	0.980	0.863	2.720(6)
5	40.80	1.645(6)	11.19	62618	1.955(8)	2.280(2)	5561	0.856	0.110	0.542	0.976	0.865	2.723(6)
6	40.56	1.724(6)	18.53	49625	2.071(8)	2.698(2)	30066	0.861	0.062	0.696	0.964	0.869	2.725(6)
7	40.21	1.738(6)	15.01	55297	2.082(8)	2.716(2)	16248	0.878	0.076	0.728	0.948	0.875	2.729(6)
8	37.86	1.328(6)	2.330	129389	2.101(8)	2.707(2)	64.2			1.	0.641	0.910	2.810(6)
9	33.37	1.212(6)	1.848	141579	2.461(8)	4.495(2)	60.3			1.	0.179	0.970	2.969(6)
10	33.26	1.205(6)	1.934	138197	2.479(8)	4.603(2)	71.1			1.	0.167	0.970	2.974(6)
11	33.12	1.205(6)	2.170	130647	2.504(8)	4.748(2)	103.9			1.	0.152	0.702	2.979(6)

order modes of models 5, 6, and 7, probably on account of the high density contrasts of these models. Therfore we have computed long series of adjacent modes, up to p-modes of order about thirty. For these high order modes, the usual criterion of classification seems to work properly. Then, step by step, it was possible to assign their correct names to all the modes of the series.

Table 2 gives the periods of a few modes, selected as the best candidates for vibrational instability.

4. Vibrational stability

The influence of the non conservative terms is estimated through a damping coefficient σ' such that the perturbed displacement $\delta \boldsymbol{r}$ is proportional to $\exp(-\sigma' t)$. This coefficient takes the form (Ledoux, 1969)

$$\sigma' = -\frac{1}{2\sigma_a^2} \frac{\int_0^{Ma} \frac{\delta T}{T} \delta\varepsilon \, dm - \int_0^{Ma} \frac{\delta T}{T} \delta\left(\frac{1}{\varrho} \nabla \cdot \boldsymbol{F}\right) dm}{\int_0^{Ma} \delta \boldsymbol{r} \cdot \delta \boldsymbol{r} \, dm} = -\frac{E_N - E_F}{D}. \quad (1)$$

The terms appearing in the right hand member of Eq. (1) are computed with the help of the adiabatic eigenfunctions obtained in Sect. 3. Their detailed expressions can be found for example in Gabriel et al. (1975).

Table 2 gives the vibrational stability results for the models quoted in Fig. 1 and Table 1. A negative sign for σ' means vibrational instability. We have investigated here the first g^+ modes of harmonics degree $l = 1$.

Let us start the discussion by considering the behaviour of the eigenfunctions. Figure 3 shows the perturbation of the pressure $\delta P/P$ corresponding to the g_1^+, g_2^+, and g_3^+ modes in models 2, 3, 4, and 5 as a function of the radius r/R. As in the radial case, the nuclear term E_N is always destabilizing and its magnitude depends on the amplitude of $\delta T/T$ or $\delta P/P$ in the nuclear burning region, while, in the models studied here, the flux term E_F is stabilizing and the more important as the amplitude of $\delta P/P$ in the external layers is large. In the case of non radial eigenfunctions $\delta P/P$ goes to zero as r^l near the center, which means that core burning models will generally have E_N terms much smaller than in the radial case.

In Fig. 3, the hatched zones represent nuclear burning regions. Let us examine the eigenfunctions in model 2. $\delta P/P$ shows a sharp extremum centered at $r/R \sim 0.4$ and a small amplitude in the external layers. But, as model 2 is still a core H burning model, it is clear that the situation is not at all favourable for an instability of nuclear origin. The situation is even worse for the g_2^+ mode whose surface amplitude is larger. Turning to model 3, one can see that the extremum has moved closer to the center, while a H burning shell has developed just in the maximum amplitude region. Since the amplitude of $\delta P/P$ at the surface remains small, the E_N term overcomes the E_F term and this model is unstable with an e-folding time of the order of 1800 yr. In the case of the g_2^+ mode, the node in $\delta P/P$ takes place inside the H burning shell, so the nuclear term is smaller, model 3 is stable towards the g_2^+ mode. Let us now discuss model 4. In the case of the g_1^+ mode, the extremum in $\delta P/P$ has come even closer to the center, so close that $\delta P/P$ crosses the zero axis inside the H burning shell. The surface amplitude is also extremely large so this mode is definitely stable. But, turning to the g_2^+ mode, the situation is far better because, as the shell has come closer to the center, in radius, its location is just in the region corresponding to the second extremum of $\delta P/P$. As the surface amplitude is small, we obtain another case of vibrational instability. Model 4 already has a He burning core but its influence is negligible here. An interesting feature is the presence of an intermediate convective zone located in the H burning shell. As can be seen in Fig. 2, this produces a sharp decrease in the Brunt-Väisälä frequency which defines a very sharp edged region, hatched in Fig. 2, where oscillations of the eigenfunction can take place. At the same time, it prevents the eigenfunctions from oscillating in the convective zone, so the effect is very much in favour of increasing the nuclear term and thus of the occurrence of an instability. The e-folding time is here of the order of 1300 yr. The g_3^+ mode is also quite favourable here because here also the oscillations of the eigenfunction are limited to the inner part of the H burning shell with large amplitudes in the convective zone, stability in this case is only marginal. Higher order modes show similar features but the amplitudes become so large outside the nuclear burning region that the flux term E_F is dominant and those modes are stable.

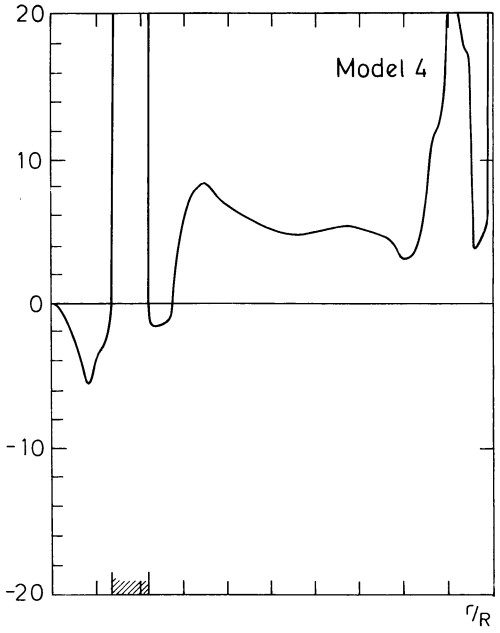

Fig. 2. Dimensionless Brunt-Väisälä frequency in model 4

A simple glance at the g_1^+ mode in model 5 shows that the amplitude is negligible in the H burning shell to this model is very strongly stable with an E_F/E_N ratio of the order of 10^5. This ratio becomes smaller as the order of the mode increases but, after a minimum value of 4.6 in the g_5^+ mode, it starts again to increase.

Up to the vanishing of the H burning shell in model 8, the same behaviour is observed, the minimum of stability being found for higher and higher order modes but these models remain stable towards the modes studied here. It is of course very unlikely to obtain an instability of this type after model 8 since nuclear burning takes place only in the core for the following evolution. The behaviour of $\delta P/P$ in g_1^+ modes along the sequence of models reflects the change in structure from a core burning model to a shell burning one and to a core burning model again. It is interesting to notice that the behaviour of $\delta P/P$ is very similar in models 1 and 9 and very different in model 5 for instance.

We can estimate the duration of the unstable phase to be of the order of 6000 yr. This is of course very short, only about 5 times

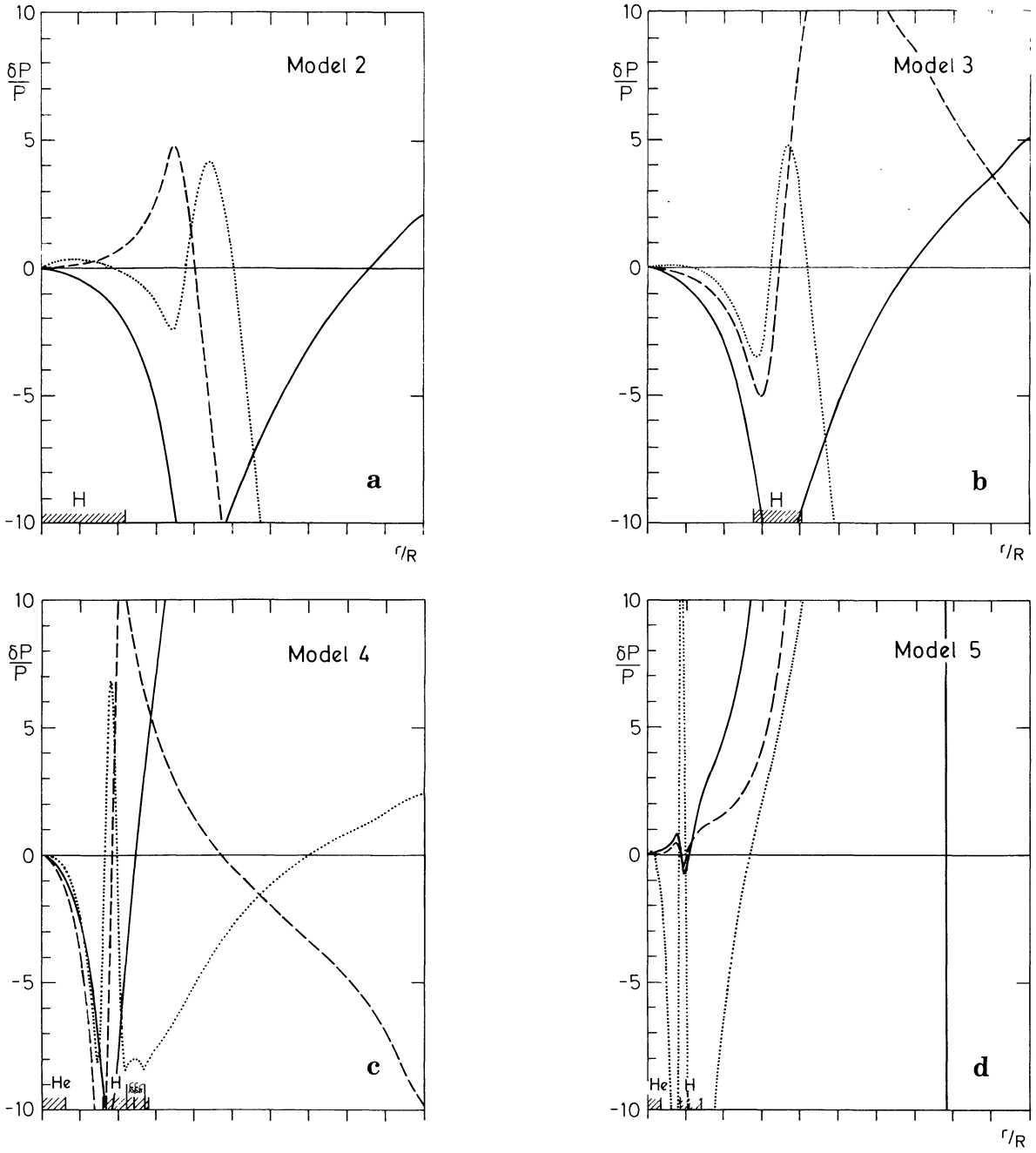

Fig. 3a–d. Relative variation of the pressure, $\delta P/P$, for $l=1$, g_1^+ (———), g_2^+ (– – – –) and g_3^+ (.....) modes. Hatchings indicate nuclear burning regions. The intermediate convective zone is also indicated in model 4

greater than the *e*-folding time. So we may not assert that this instability explains the variability observed in some WR stars. It is nevertheless interesting to notice that the periods found in this study are in accordance with the values obtained by Vreux (1985) and Vreux et al. (1985). If this instability produces an enhancement of the mass loss rate, its small duration will not drastically change the onset of the WC phase although it may of course help to shorten the WN phase. This instability may also lead to a mixing in some region of the star and if this is effective, the structure of the following models would be more homogeneous and maybe more favourable for a vibrational instability towards radial pulsations.

We cannot extrapolate these results to other values of the initial mass, we plan to analyse similar phases in less massive stars in a near future.

5. Conclusions

The important point shown up in this study is the existence of a vibrational instability towards non-radial pulsations in the evolution of a massive star, of initial mass 100 $M_\odot$, evolving with mass loss at observed rates. This instability is driven by nuclear

reactions. It starts after the exhaustion of H at the center, in models where nuclear burning takes place in a shell, distant from the center. The chemical composition at the surface is similar to a WNL star's. Those eigenfunctions having large amplitudes in the vicinity of this shell and low amplitudes at the surface are good candidates for a vibrational instability. This happens for the first g^+ modes of harmonics degree $l=1$, which have extrema of $\delta P/P$ centered on the H burning shell. The presence of an intermediate convective zone, preventing the eigenfunctions from oscillating in the nuclear burning region is a favourable factor for such an instability. When core He burning becomes important, the transition from H shell burning to core He burning modifies the behaviour of the eigenfunction and stability is restored. Core He burning models have eigenfunctions, for the first g^+ modes, very similar to core H burning models. These WNE and WC models remain stable, nuclear burning taking place near the center where the amplitudes go to zero. The effects of such an instability are difficult to estimate. The *e*-folding time is of the order of 1000 yr but the whole duration of the unstable phase is only about 5 times more. So, it is somewhat difficult to explain an observable variability by such a short growth in the amplitude. We may suggest that this would contribute to an enhancement of the mass loss rate, which would help to increase the duration of the WC phase. Another hypothesis is that it causes a partial mixing, making the structure more homogeneous and thus more likely to become unstable towards radial pulsations.

References

Boury, A., Gabriel, M., Noels, A., Scuflaire, R., Ledoux, P.: 1975, *Astron. Astrophys.* **41**, 279

Boury, A., Ledoux, P.: 1965, *Ann. Astrophys.* **28**, 353

Fowler, W.R., Caughlan, G.R., Zimmerman, B.A.: 1975, *Ann. Rev. Astron. Astrophys.* **13**, 69

Gabriel, M., Scuflaire, R.: 1979, *Astron. Astrophys.* **29**, 135

Gabriel, M., Scuflaire, R.: 1980, in *Nonradial and Nonlinear Stellar Pulsation*, eds. H.A. Hill, W.A. Dziembowski, Springer, Berlin p. 478

Gabriel, M., Scuflaire, R., Noels, A., Boury, A.: 1975, *Astron. Astrophys.* **40**, 33

Huebner, W.F., Merts, A.L., Magee Jr. N.H., Argo, M.F.: 1977, Astrophysical Opacity Library, Los Alamos Scientific Laboratory report LA-6760-M

Ledoux, P.: 1969, in *La Structure interne des Etoiles*, XIe cours de perfectionnement de l'Association vaudoise des Chercheurs en Physique, Saas Fee, p. 44

Maeder, A.: 1985, *Astron. Astrophys.* **147**, 300

Noels-Grötsch, A.: 1967, *Ann. Astrophys.* **30**, 349

Noels, A., Gabriel, M.: 1981, *Astron. Astrophys.* **101**, 215

Noels, A., Gabriel, M.: 1984, Proc. 25th Liège Int. Astrophys. Coll., 59

Noels, A., Magain, E.: 1984, *Astron. Astrophys.* **139**, 341

Noels, A., Masereel, C.: 1982, *Astron. Astrophys.* **105**, 293

Osaki, Y.: 1975, *Publ. Astron. Soc. Japan* **27**, 237

Scuflaire, R.: 1974, *Astron. Astrophys.* **36**, 107

Simon, R.: 1957, *Bull. Acad. Roy. Belgique, Cl. Sci.* **43**, 610

Simon, N.R., Stothers, R.: 1969, *Astrophys. J.* **155**, 247

Simon, N.R., Stothers, R.: 1970, *Astron. Astrophys.* **6**, 183

Stothers, R., Simon, N.R.: 1970, *Astrophys. J.* **160**, 1019

Vreux, J.M.: 1985, *Publ. Astron. Soc. Pacific* **97**, 274

Vreux, J.M., Andrillat, Y., Gosset, E.: 1985, *Astron. Astrophys.* **149**, 337

Weller, W.G., Jeffer, S.: 1979, in *Mass Loss and Evolution of O-type Stars*, IAU *Symp.* **83**, eds. P.S. Conti, C. de Loore, p. 27